Journal of Hydrology 633 (2024) 130935

Contents lists available at ScienceDirect

Journal of Hydrology

journal homepage: www.elsevier.com/locate/jhydrol

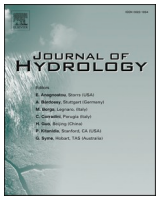

Research papers

Temporal shift of hydroclimatic regime and its influence on migration of a high latitude meandering river

Linnea Blåfield [a,*], Hannu Marttila [b], Elina Kasvi [a], Petteri Alho [a,c]

[a] Department of Geography and Geology, University of Turku, Vesilinnantie 5, FI-20014 Turku, Finland
[b] Water, Energy and Environmental Engineering, Faculty of Technology, University of Oulu, Pentti Kaiteran katu 1, FI-90014 Oulu, Finland
[c] Finnish Geospatial Research Institute FGI, Vuorimiehentie 5, FI-02150 Espoo, Finland

ARTICLE INFO

Keywords:
Boreal hydrology
Climate change
Hydroclimatic regime
Meander migration
Fluvial geomorphology

ABSTRACT

Climate change alters high latitude hydrological cycle by diminishing the snow accumulation and spring flood magnitude, and by altering temperature and rainfall finally leading to hydroclimatic regime shift from snow-dominated to rain-dominated. These changes in temperature, precipitation patterns, and discharge strongly influence geomorphological processes in fluvial environments, leading to alterations in sediment transport, erosion, accumulation, and landscape changes. We conducted comprehensive analysis of hydroclimatic trends and shifts on boreal Oulanka River system, spanning over the past five decades. A strong signal of warming temperatures (+0.61 Celsius/decade), reduced winter conditions and warmer summers (+0.41 Celsius/decade) was detected. The spring flood magnitude diminished 7 %, but high discharge peaks (Q > annual p90m^3/s) during other seasons increased 22 % together with 28 % increase of annual minimum discharge. Simultaneously, precipitation intensity increased during summer. The meander migration rate (mean 0.89 or 2.55 m/year) and bank erosion volume were interconnected to ground frost, high snow sum, high discharge, and high-water level during spring flood, but no significant long-term trends were observed. Our findings underscore that climate is the first-order control on fluvial geomorphology and emphasizes the complex interplay between various hydrological and climatic factors that shape the dynamics of river systems. Based on the results, we expect to see changes in the spatial–temporal distribution of high latitude rivers sediment flux in future. In addition, more attention should be addressed to the thaw seasons controlling the sediment transport, as majority of the observed shifts took place in these months.

1. Introduction

High latitude regions are considered highly vulnerable to climate change impacts (IPCC, 2022), and face magnitude faster temperature increase than global average (Rantanen et al., 2022). Several studies have already confirmed the rapid changes of hydroclimatic and geomorphological factors at high latitudes (Bieniek et al., 2018; Brown et al., 2018; Niittynen et al., 2018; Mustonen and Shadrin, 2021) e.g., changes in hydrological cycle and patterns, snow cover accumulation and duration, ice thickness, and river erosion. The ongoing global warming is expected to affect these factors with accelerating rate (Veijalainen et al., 2010; Box et al., 2019; Sippel et al., 2020). Since climate is typically considered as the first-order control to hydrology, the changes in hydroclimatic conditions are reflected to fluvial geomorphology as changes in sediment flux and landscape erosion (Bergström et al., 2001; Lane et al., 2007; Devito et al., 2005; Kociuba et al., 2012; Meriö et al., 2019).

Especially in snow-dominated boreal hydrology, the shift from snowfall to rain and earlier snow melting in spring will have significant impact on water storages inside the catchment areas, and to the timing and magnitude of discharge events in rivers (Woo et al., 2008; Veijalainen et al., 2010; Stocker et al., 2013; Berghuijs et al., 2014; Laudon et al., 2017; Blöschl et al., 2017; Jenicek et al., 2018; Irannezhad et al., 2022). Many studies have recognised the role of high discharges during spring flood as the main factor controlling the sediment erosion and transport in snow-dominated areas (Lane et al., 2007; Lotsari et al., 2010) as the snowpack and thermal conditions determine the timing, magnitude, and duration of the spring flood (Cockburn and Lamoureux, 2008). In addition, frequency and intensity of extreme rainfall events in Fennoscandia is expected to increase (Jonasson and Nyberg, 1999;

* Corresponding author.
E-mail address: linnea.m.blafield@utu.fi (L. Blåfield).

https://doi.org/10.1016/j.jhydrol.2024.130935
Received 30 June 2023; Received in revised form 11 December 2023; Accepted 13 December 2023
Available online 29 February 2024

Veijalainen et al., 2010), especially during late summer (Favaro and Lamoureux, 2014). The increasing precipitation have the potential to mobilize considerable amounts of sediment through increased runoff and higher discharges (Lamoureux, 2000; Lewis et al., 2019).

River bank erosion is one of the major sources of riverine sediment and in general the bank erosion processes are well understood and documented (Thoma et al., 2005; De Rose & Basher, 2011; Hughes et al., 2022). The stream power increases when the water volume, flow velocity, and depth increase. Thus, it is necessary to consider not only the changes in hydroclimatic, but also in the geomorphological aspects of fluvial environments, when evaluating the climate change impacts (Li et al., 2021). If the timing, magnitude or frequency of peak discharges changes due to climate change, it will also alter the erosion and sediment transport processes. Sediment redistribution is the main driver for landscape development, and it is an important indicator of the river system functioning and stability (Walling, 2009; Beel et al., 2018; Li et al., 2021). Changes in sediment flux can result in major impacts on e.g., stability of the channel, channel characteristics, nutrient cycle, and degradation of fluvial habitats. Currently, models for climatological, hydrological and vegetational future scenarios, have been systematically ignoring the impact of climate change on geomorphology (Goudie, 2006; Lane, 2013). Therefore, the climate change impact on fluvial geomorphology should be a major research priority and there is a need to document long existing time series from hydrological and geomorphological changes in high latitude conditions.

In meandering rivers, bank erosion is associated with lateral migration of meanders over time. However, the lateral migration of confined meanders is restricted by the narrow valley confinement. This leads to meanders migrate downstream as a coherent waveform, curvature remaining relatively constant through time (Nicoll and Hickin, 2010). The meander bend characteristics such as planform type, sinuosity, wavelength, and curvature are proven to have significant impact on erosion volume and migration rates (Lotsari et al., 2014; Salmela et al., 2020). In long-term, these characteristics are controlled by hydroclimatic conditions such as flow regime and long-term climate trends e.g., spring flood, precipitation, and snow accumulation (Leopold & Wolman, 1960; Hooke, 2008; Kasvi et al., 2013). Therefore, we can expect the changing hydroclimatic conditions to influence geomorphological characteristics of meandering rivers and the landscape.

Previous studies have also emphasized temperature as a key factor influencing sediment transport at high latitudes (Costa et al., 2018; Li et al., 2021; Syvitski, 2002; Zhang et al., 2022; Forbes and Lamoureux, 2005; Kociuba et al., 2012), as temperature influences on water amount, availability of sediment, and temporal dimensions of sediment transport. Simultaneously previous studies address the lack of well documented sedimentological data and long-time series, as well as a lack of understanding the temporal aspects of erosion and sediment transport. In the current study, we aimed to address the knowledge gap regarding the impact of climate change on fluvial geomorphology, particularly in relation to erosion volume and migration rate of meanders. Our study gathered field measurements of erosion and retreat rates for two riverbanks of 49-year time series and combined it to old aerial photographs. This overcame the challenges associated with relying solely on aerial photography, which can lead to errors due to substantial time gaps.

The study followed three main approaches. First, we examined hydroclimatic trend and shifts from 1974 to 2022 to assess how global warming has affected the hydroclimatic conditions of the Oulanka River area. Secondly, we analysed meander erosion and migration data from 1975–2022, to identify any changes or trends in erosion and migration rates of the channel. Finally, we analysed linkages and possible causal connections between hydrological, climatological, and geomorphological variables. We expect the climate change impact to be visible in the meteorological time series, and to detect changes in the timing of hydrological events. The geomorphology i.e., migration rate and erosion volume of the riverbanks, are expected to react to the ongoing hydroclimatic change.

2. Study site

The free-flowing Oulanka River locates in the NE Finland (Fig. 1). The river and its catchment are protected by Oulanka National Park, established in 1956. Oulanka River's characteristics are well described by its name, which literally means "a flooding river." This is firstly due to the small lake proportion (4,7 %) of the catchment, high proportion of peatlands (40 %), catchment topography and the fact that Oulanka area is known as the snowiest region of Finland (Kersalo & Pirinen, 2009). The snowmelt driven spring flood usually takes place from mid-May to mid-June, and is measured to be up to 155 times larger than the minimum discharge. The 135-kilometre-long channel discharges into Lake Paanajärvi and finally to the White Sea.

The river flows in a canyon-like bedrock formations apart from the downstream section, which meanders in a 1-kilometre-wide bedrock valley filled with glaciofluvial deposits. The river has eroded its channel 40-metres deep into these valley deposits creating terraces and oxbow lakes. Because of the narrow valley configuration, the river cannot expand in a lateral direction, therefore erosion causes meanders to migrate downstream. The migration rate is measured to be one of the fastest in Fennoscandia (Koutaniemi, 2000). Simultaneously the sinuosity values of the meanders are relatively low due to the degree of confinement.

The continental climate causes large temperature fluctuations from −48 °C, up to +32 °C, the annual mean temperature of the area being 0 °C (Pirinen et al., 2012; Jokinen et al., 2021). Winter is the dominant season lasting for 6 months, while other seasons are short but distinct. The alternating terrain elevations affect the amount of rainfall and snow. The mean annual precipitation of the region is 550 mm of which half falls as snow between October and May. Ground frost is present from October to mid-June, and it can reach the depth of 0.4–1 m (Koutaniemi, 1984).

The observed banks are located within 4-kilometer distance from each other (Fig. 1). The channel slope between the observed banks is 0,21 m/km. Bend and bank 1 locates at the narrowest section of the valley, occupying the whole 600-meter valley width. At present, bend 1 has a rm/w ratio of 4,5, sinuosity of 1,89, slope of 0.22 m/km, and a channel width of 30 m during mean Q, and 120 m during bankfull discharge. The outer bank of bend 1 is 450 m long and 3 to 7 m in height. D50 particle size of the bank1 ranges from 0,18 mm to 46 mm. The bank soil is rich with pebbles and cobbles of size up to 80 mm. The main textural groups of the bank are gravel and gravelly sand. At bend 2, the valley width widens to 1.1 km. At present, the bend has a rm/w ratio of 3,3, sinuosity of 1,4, slope of 0.33 m/km, and a channel width of 45 to 150 m (mean Q/bankfull). The outer bank of bend 2 is 300 m long and 3 to 5 m in height. D50 particle size of bank 2 ranges from 0,2 mm to 33 mm, pebbles and cobbles are sparsely found. The main textural groups of the bank are slightly gravelly sand and gravelly sand. Both vertical banks lack vegetation, but on top of the banks there are coniferous forest and a thick layer of mosses and lichen, which are overhanging and collapsing on the banks as the banks erode.

3. Data and methods

3.1. Monitoring of the area

Geomorphology of the Oulanka River was actively studied between 1975 and 1995 by Koutaniemi (1979; 1984; 2000). These measurements were then paused until the Oulanka Research Station (University of Oulu, Finland) restarted them continuously from 2008 onwards. At the research station there is a weather and discharge station, both operating since 1966. Historical aerial photographs were taken by different parties with 1-to-10-year gaps. From 2004 onwards geometrically corrected orthophotos from the area have been produced by the National Land Survey of Finland (NLS). From 2020 onwards, regular geomorphological monitoring with state-of-the-art technology has been carried out on the

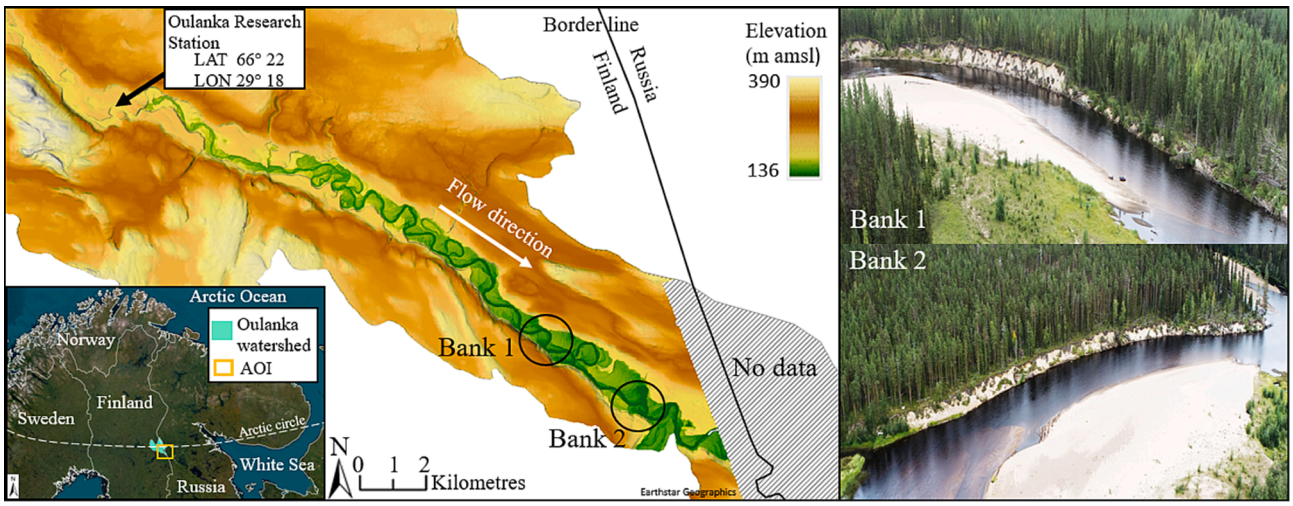

Fig. 1. Location of Oulanka River catchment, area of interest (AOI), meander bends, and the weather and discharge station. Aerial photos of Bank 1 and Bank 2 in were taken in autumn 2022. The discharge and weather station are located at the Oulanka Research Station.

area. Temporal dimensions of the data in Fig. 2.

3.2. Hydroclimatic observations

Permanent discharge and weather stations, operating since 1966, are located at the Oulanka research station approximately 14 km upstream from the area of interest. Discharge and water level data is measured hourly, and the data is openly available in the Finnish Environment Institute (SYKE) database. In this study, daily minimum discharge (MinQ), mean discharge (Mean Q), maximum discharge (Max Q), and daily mean water level data from January 1974 until December 2022 (49 years) was analysed to determine the monthly and annual flow characteristics as well as long-term trends and shifts. Multiple variables (Appendix 1) were derived from these main records to assess the timing, duration, magnitude, and proportion of different discharge and water level phenomenon, both, monthly and annually. In this study, the spring flood (SF) was defined as the 90th percentile (p90) of the annual discharge values. Duration and magnitude of spring flood were calculated by determining the number of days between $Q > p90$ and $Q < p90$. Flooding on other seasons was defined as $Q > p90$ outside the spring flood.

The meteorological station measures multiple weather parameters and the data is openly available in Finnish Meteorological Institute's (FMI) database. In this study the daily data of temperature (Min T, Mean T, Max T), precipitation (P) and ground frost (GF) were used for the period of 1974–2022 to analyse possible trends and shifts. Multiple variables (Appendix 1) were derived from the main records to assess the duration, magnitude and timing of meteorological phenomenon. The meteorological station locates 248 meters above mean sea level and approximately 100 meters higher than the meanders of interest.

3.3. Field measurements in 1975–1995: Geometric levelling

Geomorphological observations of Oulanka River started in 1975 to determine erosion volume and migration rate of the outer banks, and the erosion and deposition volumes of point bars (Koutaniemi, 1979; 1984). The first 6-year monitoring period (1975–1981) was carried out in both bends, but the next 11 years of monitoring (1985–1995) focused only on bend 1, since it was behaving more like a classic meander (Koutaniemi, 2000). In the first measurement campaign a total of 9 markers were installed on top of both outer banks with 30-meter intervals and 5-meter distance from the bank edge. For the later monitoring period the number of markers was increased from 9 to 16 at bend 1 with an interval of 15 m. This enabled denser measurement interval and therefore more accurate estimation of the erosion volume and retreat rate. The distance from the bank edge to the markers on top of the banks was measured annually every autumn.

AGA EDM Geodimeter Model 76 was used to measure migration rate of the banks and volumetric changes on the point bars. The distance between a solid benchmark on the upper point bar and the upper margin of the outer bank was measured annually every autumn. The measuring intervals were similar to the markers on the top of the banks. Changes of distance between solid benchmark and bank margin enabled trigonometric calculations of migration of each point in direction of the longitudinal axis of the valley. Simultaneously, elevation changes on point bars were measured along the 9 or 16 marker lines with 12-meter longitudinal interval from vegetation line until the water.

3.4. Field measurements in 2020–2022: Terrestrial laser scanning

In field campaigns of 2020–2022 the geomorphological measurements were conducted using Riegl VZ-400 3D Terrestrial Laser Scanner (TLS).This scanner operates in the shortwave near-infrared spectrum

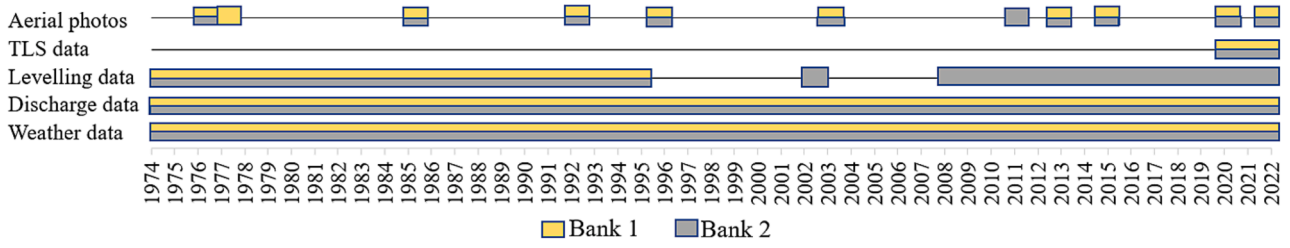

Fig. 2. Temporal dimensions of the data set used in this study. TLS = Terrestrial Laser Scanner.

(1550 nm) and has a laser pulse repetition rate of up to 300 kHz. The accuracy of the scan data acquisition is 5 mm, with a repeatability of 3 mm. The scanner was equipped with an inclination sensor, an internal compass, a GPS receiver for positioning, and a camera for colorizing the point cloud. The scanner and its instruments are regularly calibrated by the manufacturer.

During the campaigns, the scanner was operated in a mode, which has a beam footprint of 0.04 m at a distance of 100 m. To georeference the point cloud, eight targets with a diameter of 0.05 m were placed around the area and their precise x, y, and z coordinates were measured using an VRS-GNSS. Each scan was conducted in a way that at least three mutual targets from subsequent scans were registered. The measurements in each campaign were implemented identically.

3.4.1. TLS point cloud processing

The scanned point clouds were registered into a local coordinate system (EUREF-FIN TM35FIN) using Riegl's RiSCAN PRO® software package. The measured targets served as tie-points between individual point clouds, allowing the scans to be combined and aligned in a coordinate system based on the x, y,z coordinates of the targets. Rotation and translation errors were corrected using a multi-station adjustment (MSA) approach, which iteratively modified the orientation and position of each point cloud. The point cloud was then filtered to reduce noise and extract unnecessary objects, such as trees. The final point density of the point clouds ranged from 100 to 1000 points per square meter.

Further processing of the point clouds was performed using an open-source software Cloud Compare (v2.12.4). The remaining vegetation was filtered out using the CANUPO-plugin, which classifies the point cloud based on user-defined and trained classifiers, providing a confidence value for each point. In this study, vegetation was filtered from the cloud using a trained classifier with a confidence level of 0.90 % (Fig. 3). A detailed description of the vegetation filtering workflow can be found in Brodu & Lague (2012). The filtered point cloud was then used to calculate the erosion volume and bank migration rate between years 2020, 2021 and 2022.

3.5. Mapping the migration and erosion from aerial images 1976–2022

A set of historical aerial photographs and orthoimages (Table 1) were used to map the mean migration and erosion volume of the two banks over the observed time to fill the gaps with no field data. The spatial analysis of geomorphological change of banks was conducted as follows: i) georeferencing the aerial photographs, ii) mapping the upper margin of the outer bank, iii) calculating the mean migration and mean erosion volume between the images.

Table 1
Data set of aerial images. Codes: AP = Aerial photograph, OP = Orthophoto, B/W = Black and white, RGB = Red-Green-Blue band –image, NLS = National Land Survey of Finland, FDIA = Finnish Defence Intelligence Agency.

Year	Type	Colour	Scale	Source	No. of GCP	Pixel size (m)	RSME x, y (m)
1976	AP	B/W	1:31000	NLS	21	0.46	0.29
1977	AP	B/W	1:10000	FDIA	18	0.62	0.25
1985	AP	B/W	1:31000	NLS	19	0.82	0.35
1992	AP	B/W	1:61000	NLS	22	1.20	0.70
1995	AP	B/W	1:61000	NLS	23	0.89	0.51
1996	AP	B/W	1:61000	NLS	23	0.40	0.40
2003	AP	B/W	1:10000	NLS	18	0.50	0.37
2011	OP	RGB	1:10000	NLS	–	0.50	–
2013	OP	RGB	1:10000	NLS	–	0.50	–
2015	OP	RGB	1:10000	NLS	–	0.50	–
2020	OP	RGB	1:10000	NLS	–	0.50	–
2022	OP	RGB	1:10000	NLS	–	0.50	–

The aerial photographs from 1976 to 1996 were georeferenced in ArcGIS Pro 3.0.3 using the following procedure; first, the area of interest was delineated in the middle of each photograph. Secondly, several ground control points (GCP) were manually added on each photograph, based on visual identifiers, and referenced to the 2022 orthoimage. The GCP's were added evenly on both sides of the channel on the river margins. Since the homogeneous distribution of GCP's was difficult, a first order polynomial function was used for rectifying the photographs as it works well on flat surfaces like floodplains, and it presents more conservative errors between GCP's than nonlinear adjustments would (Gurnell, 1997).

The mean bank migration, and the mean erosion volume of the banks were calculated for time periods between the images. Several factors effected whether the upper margin could be confidently mapped from the images: (i) image resolution, (ii) shadows and sun reflections, (iii) high vegetation on riparian. The mapping resulted in several polylines representing the upper margin of the bank at each image interval. The mean migration rate between images was calculated from the horizontal distance of neighbouring polylines. Erosion volume was estimated based on the margin retreat, bank height and vertical surface area.

3.6. Statistical analyses

Time series of 49 years including a total of 46 different hydrological,

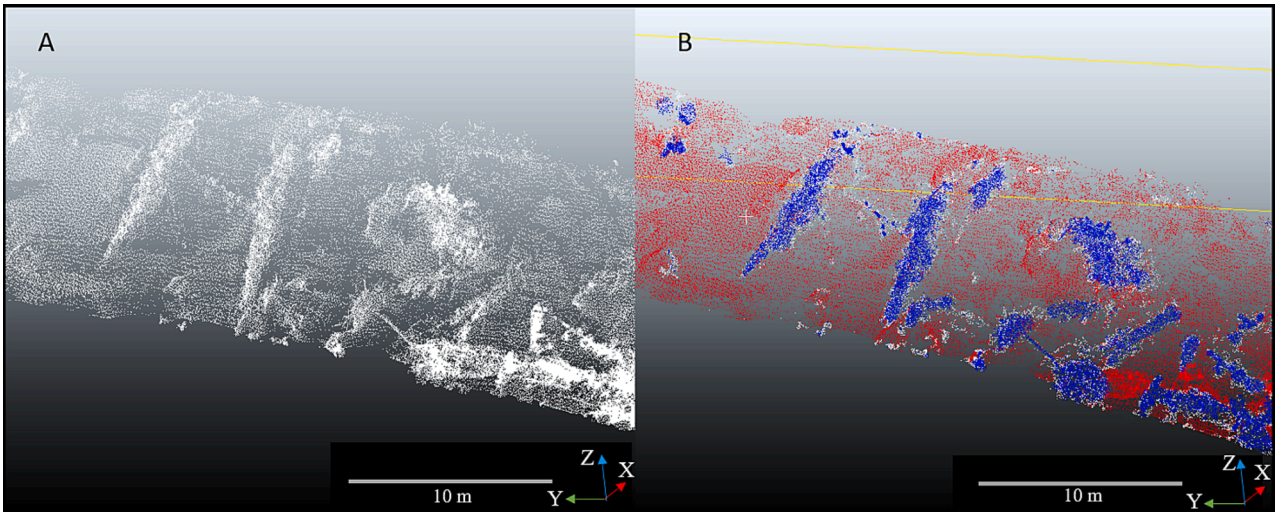

Fig. 3. A section of bank 1 TLS point cloud. A) Raw point cloud. B) CANUPO-classified point cloud. Red points are classified as ground, blue point as vegetation, and white points as uncertain. (For interpretation of the references to colour in this figure legend, the reader is referred to the web version of this article.)

meteorological, and geomorphological variables (Appendix 1) were statistically tested using the XLSTAT-program. First, the long-term trends were analysed using the Mann-Kendall trend test (Mann, 1945; Kendall, 1975), which is a non-parametric, rank based test determining possible statistically significant trends in a time series.

In this study, the Mann-Kendall (M−K) trend test was carried out on all variables of the hydrological, meteorological, and geomorphological time series with $\alpha = 0.05$ significance level identifying statistically significant trends. Possible serial correlation increases the chance of trend being significant, therefore this effect was removed by using Hamed & Rao (1998) M−K modification, which is explained in detail in e.g., Daneshvar Vousoughi et al., 2013; Dinpashoh et al., 2011; Jhajharia et al., 2014; Partal and Kahya, 2006. The effect of outliers on the trend was neglected by using a non-parametric linear regression Sen's slope estimator (Sen, 1968; Daneshvar Vousoughi et al., 2013; Dinpashoh et al., 2011; Jhajharia et al., 2014; Partal and Kahya, 2006).

Secondly, the possible shift points of hydrological and meteorological variables were analysed using the non-parametric Pettitt test (Pettitt, 1979), which has been used in number of hydroclimatological studies to detect significant changes in the time series mean (Wijngaard et al., 2003; Verstraeten et al., 2006; Zhang and Lu, 2009; Villarini and Smith, 2010; Liu et al., 2012; Wu et al., 2019; Citakoglu & Minarecioglu, 2021). It is based on Mann-Whitney two-sample test (rank-based) which allows the detection of single shift at an unknown point in time series. Pettitt test is not specifying the distributional assumptions, and therefore it may be inefficient in detecting breaks of extremes, but simultaneously makes the test non-sensitive to outliers (Xie et al., 2014; Li et al., 2016).

In this study, the null hypothesis was: No change in the distribution of the variable i.e., the data is homogeneous. The alternative hypothesis was that the distribution of the variable differed i.e., there is a significant change in the data. Significance level was 5 %, and the p-values were calculated using the Monte Carlo approach with confidence interval of 99 %. Since the study area locates in a national park, and the measuring stations have been constant through the time series; the human intervention to river flow is minimal. Hence, we can assume that the possible shift points are natural and climatic driven.

Thirdly, the possible correlations between variables were tested using the Spearman's rank coefficients (Spearman, 1906), which is a non-parametric test which measures the strength and direction of monotonic relationships between paired variables. Furthermore, in this study, the focus was on detecting the hydrological and meteorological variables which correlate with the geomorphological variables; erosion volume and migration rate. In addition, partial correlation coefficient analyzis (Iman and Helton, 1988) was run to eliminate the influence of covariates.

4. Results

4.1. Hydroclimatic trends

An overall increase of temperature and rapidly reduced winter conditions were detected from the analysis of temperature related variables. Monthly mean temperatures increased by 1 to 7 degrees of Celsius (℃), where as annual mean temperature increased by 3.05 °C over the period of 1974–2022, indicating 0.61 °C increase annually/decade (Table 2). The most significant warming trend was observed during winter months from October to March, being 3.48 °C on average and 0.69 °C annually/decade (Table 2). Diurnal Temperature Range (DTR) decreased 2.4 °C, indicating a reduction of temperature range between daily minimum and maximum values (Fig. 4). Furthermore, significant trends were observed in various temperature-related variables, including annual frost sum (−39 %/−760 °C), number of ground frost days (−6 %/−9 days), number of snow cover days (−6 %/−13 days), number of frost days (−7 %/−13 days), and the timing of thermal spring (−16 %/−19 days) (Fig. 4).

Annual mean precipitation increased by 1.8 %/9.3 mm or 1.86 mm per decade, however the trend was not significant (Table 2). In monthly data, summer precipitation showed significant increase, while thaw-season e.g., November and March experienced significant decrease (Table 2). Simultaneously, the number of precipitation days decreased by 14 %/−28 days (Fig. 4), indicating an increase in precipitation intensity rather than in event frequency. The annual snow sum decreased by −11 %/−1020 cm, which is potentially caused by larger amount of precipitation falling as rain instead of snow, and properties of the snow itself e.g. density or snow water equivalent.

Total magnitude of spring flood (SF) decreased by 4 %, likely due to reduced snow accumulation. Simultaneously, the proportions of SF and annual p90 total volume decreased from the annual Q volume (-7 % and -10 %, respectively) (Fig. 4). In addition, changes in timing and duration of SF were detected as the discharge rising and falling above/below the annual P90 stage shifted to earlier, and the time between the rise and fall shortened. The increase of monthly Mean, Min, and Max Q values in April and May, and their decrease in June supports the change in timing (Table 2). This can be attributed to higher spring temperatures, resulting in an earlier onset of thermal spring, and earlier melting of ice and snow. Despite the decreased SF magnitude, the number of p90 flood peaks outside of SF increased by 22 %. This is potentially caused by the increased precipitation and runoff outside of spring, as well as the prolongation of the period in which precipitation falls as rain instead of snow.

The range between discharge extremities decreased as the annual Min Q increased by 28 %, while there was no significant trend observed in the annual Mean or Max Q (Table 2). The increased Min Q led to an increasing trend of the annual discharge volume, however, the trend was not statistically significant (Fig. 4). Despite a significant decrease in November precipitation, the mean discharge in November increased significantly (Table 2). This can likely be attributed to the increased late autumn and early winter temperatures, as well as increased summer precipitation, leading to increased winter runoff from the catchment.

4.2. Shift point analysis

The Pettitt test identified significant shifts in all the hydroclimatic main variables, except in magnitude of precipitation. Earliest shift was detected in temperature related variables (Fig. 5A). Discharge and precipitation derived variables shifted with a lag of 5 to 10 years compared to temperature (Fig. 5A). Thaw-seasons experienced relatively highest number of significant shifts, whereas winter months experienced highest number of total shifts in temperature derived variables (Fig. 5B). Most of the significant shifts in monthly mean temperatures occurred between

Table 2
M−K trend test on the main variables; monthly and annual (A.) mean temperature (T), mean precipitation (P), and mean, min, and max discharge (Q). Trend per decade and total change during the time series based on Sen's slope. Bolded values were statistically significant with a P-value < 0.05.

Trend/decade	Jan	Feb	Mar	Apr	May	Jun	Jul	Aug	Sep	Oct	Nov	Dec	A.
Mean T (℃)	**0.69**	**0.51**	**0.30**	**0.48**	**0.20**	**0.23**	**0.49**	**0.51**	**0.37**	**0.50**	**0.77**	**1.41**	**0.61**
Mean P (mm)	0.04	0.10	**−1.69**	0.58	**−2.45**	0.71	**3.92**	**4.23**	−0.77	1.22	**−3.41**	**1.63**	1.86
Mean Q (m^3/s)	**0.49**	**0.53**	**0.34**	**0.86**	1.71	**−1.49**	0.46	−0.12	−0.46	0.37	**1.86**	**0.55**	0.60
Min Q (m^3/s)	**0.58**	**0.48**	**0.32**	**0.25**	**2.71**	−0.44	−0.04	0.00	−0.26	0.07	0.63	**0.40**	**0.51**
Max Q (m^3/s)	**0.40**	**0.56**	**0.41**	**2.82**	6.67	−1.85	1.52	0.00	1.13	1.23	**3.55**	0.77	2.04

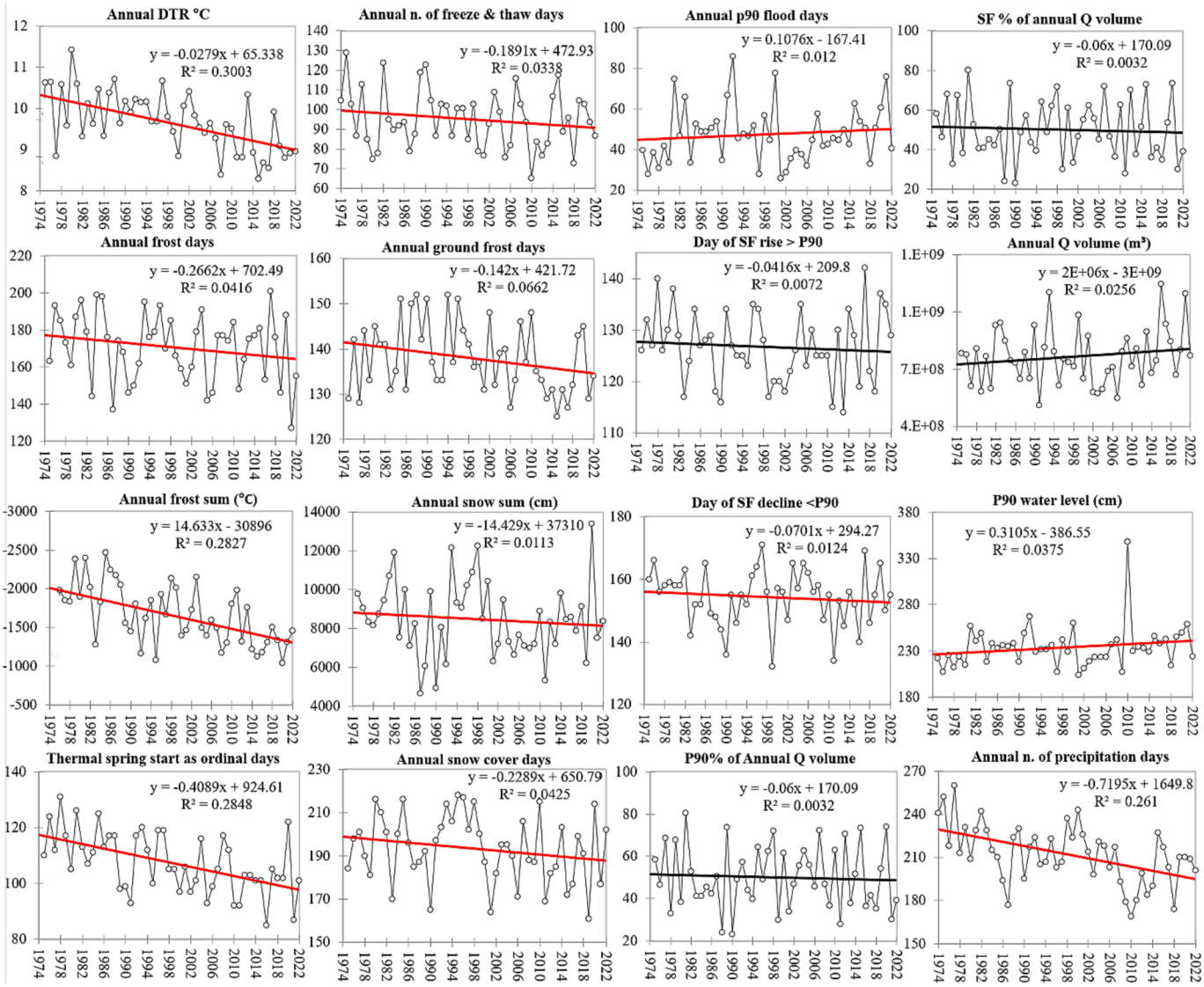

Fig. 4. M–K trend test result on relevant temperature, discharge and precipitation derived variables. Red trend line indicates significant trend, black trend line indicates non-significant trend over the time series. Days are ordinal dates. DTR = Diurnal Temperature Range, Q = Discharge. (For interpretation of the references to colour in this figure legend, the reader is referred to the web version of this article.)

1997 and 2003, indicating warmer and longer summers and autumns, as well as shorter winters (Fig. 6). Shift of annual mean temperature was detected in 2003. This shift was reflected in other temperature-derived variables such as DTR, number of frost days, timing of thermal spring, and the number of freeze–thaw days (Fig. 6). Fewer frost days in early and late winter indicated a shorter winter period, and the onset of thermal spring occurred earlier. Freeze-thaw days increased in spring and decreased in autumn.

Significant positive shifts were detected in annual Min Q as well as in monthly discharge (Min, Mean and Max Q (Fig. 6), indicating that the the variables mean value has increased abruptly. Significant negative shifts were detected in the number of precipitation days in January, September, and annual data (Fig. 6), which supports the above findings of decreased precipitation event frequency. Despite the increased trend of precipitation amount, no significant shift was found in monthly or annual precipitation amounts (Fig. 6). That is to say, we have not yet reached the culmination point of changes in precipitation amount, but it is reached in rain intensity.

4.3. Morphological change and it's relation to hydroclimatology

From the two studied banks, bank 2 migrated three times faster (on average 1.5 m faster per year) than bank 1 during the observed time series (Fig. 7A-C). Over the five decades of monitoring, bank 1 migrated a maximum lateral distance of 42 m, with an average annual migration rate of 0.89 m per year (Fig. 7B). Direction of the migration was towards downstream along the valley centre line while maintaining a constant radius of curvature and sinuosity. Bank 2 migrated a maximum lateral distance of 120 m (Fig. 7C), corresponding to an average annual migration rate of 2.55 m per year. Main direction of migration was downstream along the valley, however straightening simultaneously towards the valley centre line, leading to decrease in curvature and sinuosity.

Geodimeter measurements between 1975 and 1995 indicated that the annual mean erosion volume of bank 1 was 1859 m^3, with a range of 320 m^3 (min) and 4071 m^3 (max). For bank 2, the respective values were 3780 m^3 (mean), 1845 m (min), and 5685 m^3 (max), Subsequent TLS measurements conducted 2020-2022 indicated a net erosion volume of 4103 m^3 for bank 1 and 9310 m^3 for bank 2. Years with high snow accumulation and high discharge during spring flood (Max Q) resulted

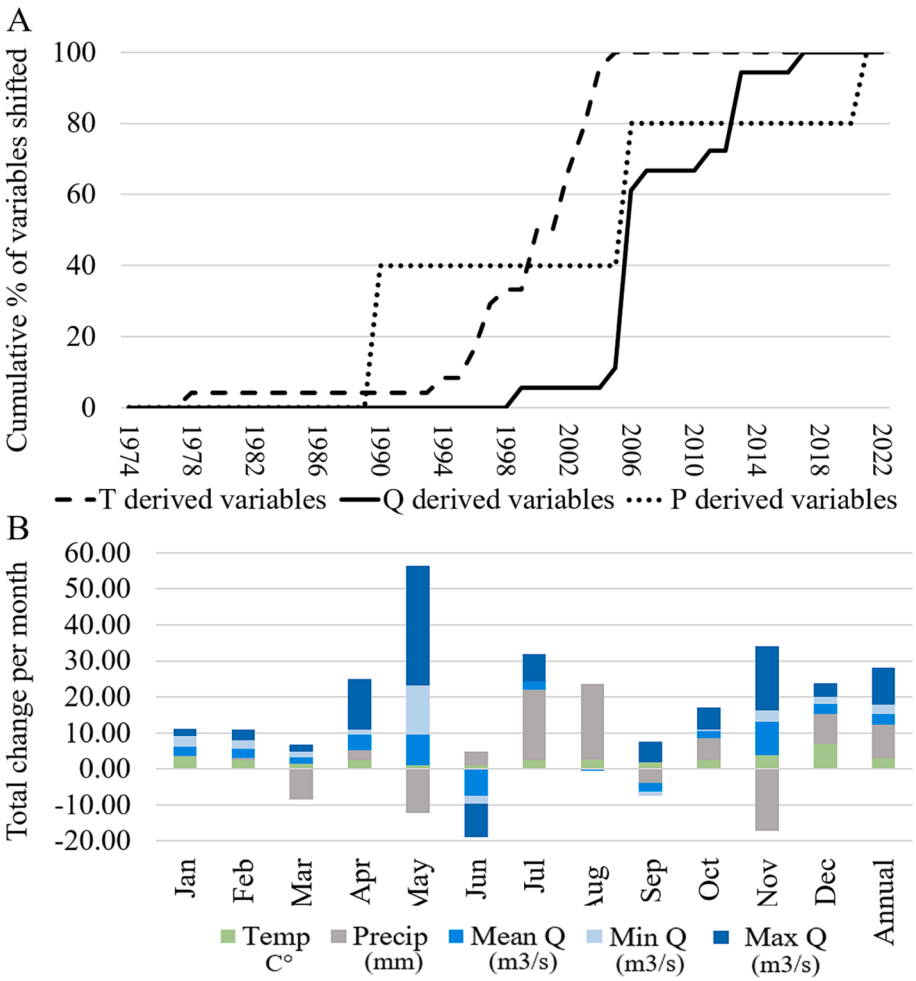

Fig. 5. A) Cumulative chart of temperature, discharge (Q) and precipitation derived variables' shift points. Temperature derived variables shifted first, majority between years 1996–2004. Discharge and precipitation variables reacted to temperature shift with a lag of ~10 years. B) Total change per month based on Pettitt test. Thaw-seasons April, May and November experienced largest number of shifts related to discharge, whereas July, August and November experienced large shift in precipitation. Winter months (Nov-Feb) experienced most changes in temperature.

the highest measured migration rates and erosion volumes (Fig. 7A). The year 2020 recorded the highest measured snow accumulation, min Q, max Q, and erosion volume of the time series. Additionally, years with above-average Min Q had also above-average bank erosion volume (Fig. 7A), indicating potentially high erosion rates even if the spring flood was of lower magnitude.

The difference in geological and topographical factors of the observed banks can generally explain the divergence in migration rates. Bank 1 has larger D50 particle size, higher vertical bank and lower slope than bank 2 which makes bank 1 soil less erodible and decreases the erosion potential of flowing water. In addition, factors such as rm/w ratio, bankfull width of the channel, stream power and curvature are found to explain variation in migration rates (Richard et al., 2005; Nicoll & Hickin, 2010). Maximum migration rates are generally found with rm/w ratio of 2 to 3, which could explain bank 2 was migrating faster than bank 1. In addition, bank 2 has larger bankfull width which is commonly attributed to stronger stream power, potentially leading to more intense erosion. These factors support the above findings of different migration rates.

Correlation analysis between geomorphological and hydroclimatic variables indicated correlation between erosion volume and snow sum, Max Q and Min Q (Appendix 2). Migration rate correlated strongest with the max Q, maximum water level (Max WL), and spring flood volume (Appendix 2). Min Q particularly explained the migration rate and erosion volume in years with low Max Q. Partial correlation test with a threshold of 0.95 indicated that number of ground frost (GF) days was the sole parameter controlling erosion volume when excluding the effects of covariates. Lowering the threshold to 0.80 revealed partial correlation between erosion volume and p90 discharge volume, Max Q, precipitation amount, and the number of flood days. Linear regression between migration rate and number of ground frost days indicated total migration rate of 46 m for bank 1, and 130 m for bank 2, which corresponds the measured values. Net volumetric change of point bars did not show any trend, neither correlation with any other variable tested, meaning irregular behaviour.

It is worth noting that none of the variables exhibited notably strong correlations or dominance over others. Although the only temperature driven variable showing correlation was the number of ground frost days, all the other correlated variables have associations to temperature as well. This supports the findings of previous studies, which highlighted the influence of temperature on the timing and magnitude of snow melt, spring floods, and winter flow, and therefore, to geomorphology (Korhonen and Kuusisto, 2010; Kociuba et al., 2012; Costa et al., 2018; Li et al., 2021). It is evident that changes in temperature, precipitation and discharge regimes, will affect the spatial–temporal magnitudes of sediment transport. Potential impacts are increased bank erosion, faster channel migration, changes in flood frequency and magnitude leading to instability of rivers.

The whole time series of the most relevant variables related to bank migration are plotted in Fig. 8. The yellow colour highlights the period

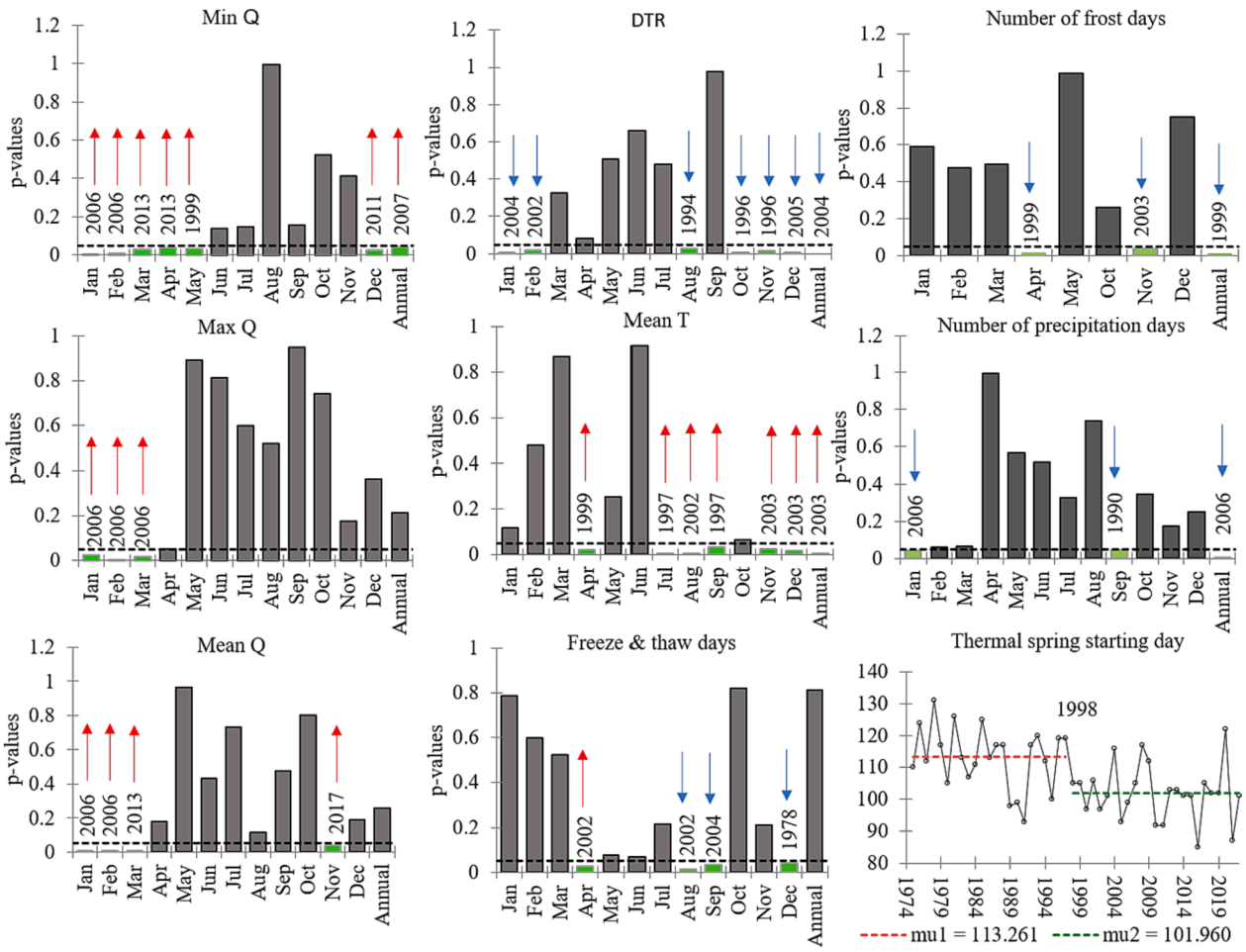

Fig. 6. Variables where significant shift point in the time series was detected. The year indicates the timing of permanent shift, and the arrow indicates either increase (red) or decrease (blue). Thermal spring mu-values represent the ordinal date of the thermal spring start before (mu1) and after (mu2) the shift. (For interpretation of the references to colour in this figure legend, the reader is referred to the web version of this article.)

where 95 % of temperature related variable means, and 65 % of discharge related variable means shifted. During this period all the discharge variables were relatively stable with no high or low peaks. Concurrently, an abrupt decrease of snow accumulation, shift of annual mean temperature from below 0 degrees Celsius to above 0 degrees Celsius, and the lowest estimated erosion and migration rates were observed. This period can be seen as a transition phase, where the river system adapted to the changing climate. It took 5 to 10 years until the shift of temperature variables was visible in the discharge variables, but no sign of geomorphological shift was detected, yet. 5-decade might be enough to detect changes in hydroclimatic regime, but sedimentological processes and landscape evolution takes much longer time, even centuries (Zhang et al., 2022).

5. Discussion

5.1. Hydroclimate

The findings of this study reinforce the understanding of rapid environmental changes in high latitudes, including decreasing snow masses, warmer temperatures and changes in hydrological regime. The fact that the shift of temperature related variables was followed by a shift of discharge and precipitation shifts with a lag of 5 to 10 years, support the results of previous studies (Bergström et al., 2001; Devito et al., 2005; Kociuba et al., 2012; Meriö et al., 2019, Gohari et al., 2022) where climate was considered as the first-order control to hydrology. The shift rate of temperature derived variables accelerated in mid-1990's reaching its maximum in 2004, which led into accelerating rate of shifts in discharge derived variables starting from 2004. This initiated transition phase of discharge variables was accompanied with relatively steady discharge phenomenon throughout the years until 2015, when the discharge started to regain high flood peaks accompanied with high base flow during winter.

The observed significant increase of flooding on others seasons than spring align with the results of Veijalainen et al. (2010) who predicted an 12–40 % increase in occurrence of flooding in other seasons by the end of the century in Finnish rivers. The results of this current study, however, indicate a more moderate decrease in SF magnitude compared to the forecasted−30 % by Veijalainen et al. (2010). This is potentially caused by the special characteristics of Oulanka catchment; above average snow fall, steep topography, high peatland proportion together with low lake percentage which result in low storage capacity and fast response of river discharge. In general, the trends and shifts detected in Oulanka river are parallel to those observed elsewhere in the high latitudes (Ahmed et al., 2020).

The decrease of discharge extremities and the significant increase of minimum discharges especially during winter align with findings reported by Korhonen and Kuusisto (2010); Duan et al., (2017); Qin et al., (2020); Irannezhad et al., (2022) and Gohari et al., (2022). During the past century, an overall increase in winter runoff due to warmer winters generating more runoff, earlier and lower spring discharge peaks, and overall reduced winter conditions were detected in Finnish rivers and in rivers across Northern Eurasia. Especially winter base flow increased in Oulanka and similar events has been interrelated with precipitation

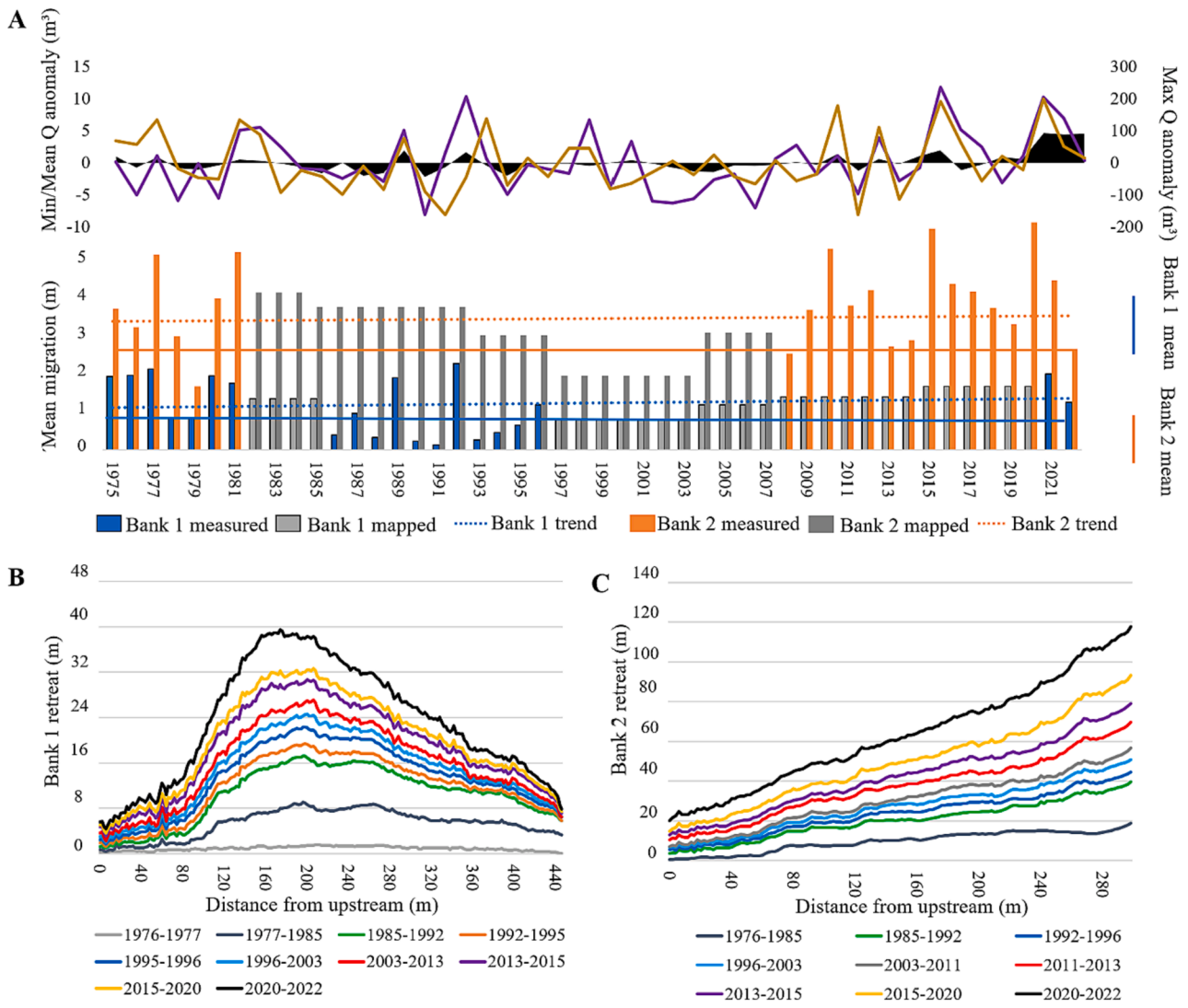

Fig. 7. Morphological change of the banks. A) Min (black), Mean (yellow) and Max (purple) Q anomaly plotted with both, measured and mapped annual migration rates of bank 1 and bank 2. Measured migration rates are based on the Geodimeter and the Terrestrial Laser Scanner data, whereas mapped migration rates are mean values for each time-interval between the aerial images. B) Retreat rates of the Bank 1 upper margin mapped from the aerial images. The bank is migrating downstream maintaining its shape. C) Retreat rates of the Bank 2 upper margin. Downstream of the bank 1 is retreating faster than the upstream.

regime shifts in Canada and Northeast Asia (St. Jacques and Sauchy, (2009; Duan et al., 2017). The pace of these trends is accelerating in Finnish and Eurasian flow regimes and has become more severe during the past 3 decades (Qin et al., 2020; Gohari et al., 2022). The acceleration of these trends was evident also in this study. If these trends continues, or accelerates even more, it is possible that we observe the −30 % decrease of SF forecasted by Veijalainen et al. (2010) also in Oulanka.

Interestingly, we did not detect decreased summer flows (June-August) (Table 2), even though previous studies (Korhonen and Kuusisto, 2010; Irannezhad et al., 2022; Gohari et al., 2022) all reported decreasing trends in summer flows across Finland. This might be due to local controlling factors on catchment scale. The steep topography and high peatland proportion of Oulanka catchment, combined with intensified and increased summer rains can potentially sustain the ecologically important summer flows in Oulanka River. In additon, the changes in hydroclimatic trends and shifts indicate a shift from snow-dominated system towards rainfall-dominated system. This perception is supported by Meriö et al. (2019), who found that the threshold zone of snow/precipitation ratio is moving northeast in Fennoscandia as the climate warms. At present, Oulanka River is at the border of this zone, meaning that there is just enough of snowmelt to recharge the summer flow, but it is close to a shift from snow-dominated to rain-dominated. Shift like this will affect not only the hydrology and geomorphology of the river system but also the whole fluvial habitat and hydroecological conditions.

5.2. *Morphology*

Both of the banks had migrated towards downstream maintaining more or less the same sinuosity, curvature and amplitude which is typical for confined meanders since they can't expand laterally (Nicoll & Hickin, 2010). However, the downstream bank 2 migrated approximately three times faster than the upstream bank 1. This difference is likely caused by the topographical and geological characteristics of the banks as bank 1 had larger particle size and lower slope than bank 2, which are apt to cause more resistance on flow and lower stream power. In addition, bank 2 had wider bankfull width which is known to cause more erosion during flooding. An increasing trend of bank erosion and migration was detected in both banks; however, this trend was not statistically significant. Despite the lack of significant shifts and trends in morphological variables, the increasing trend clearly indicates that changes in fluviogeomorphological processes in Oulanka River are

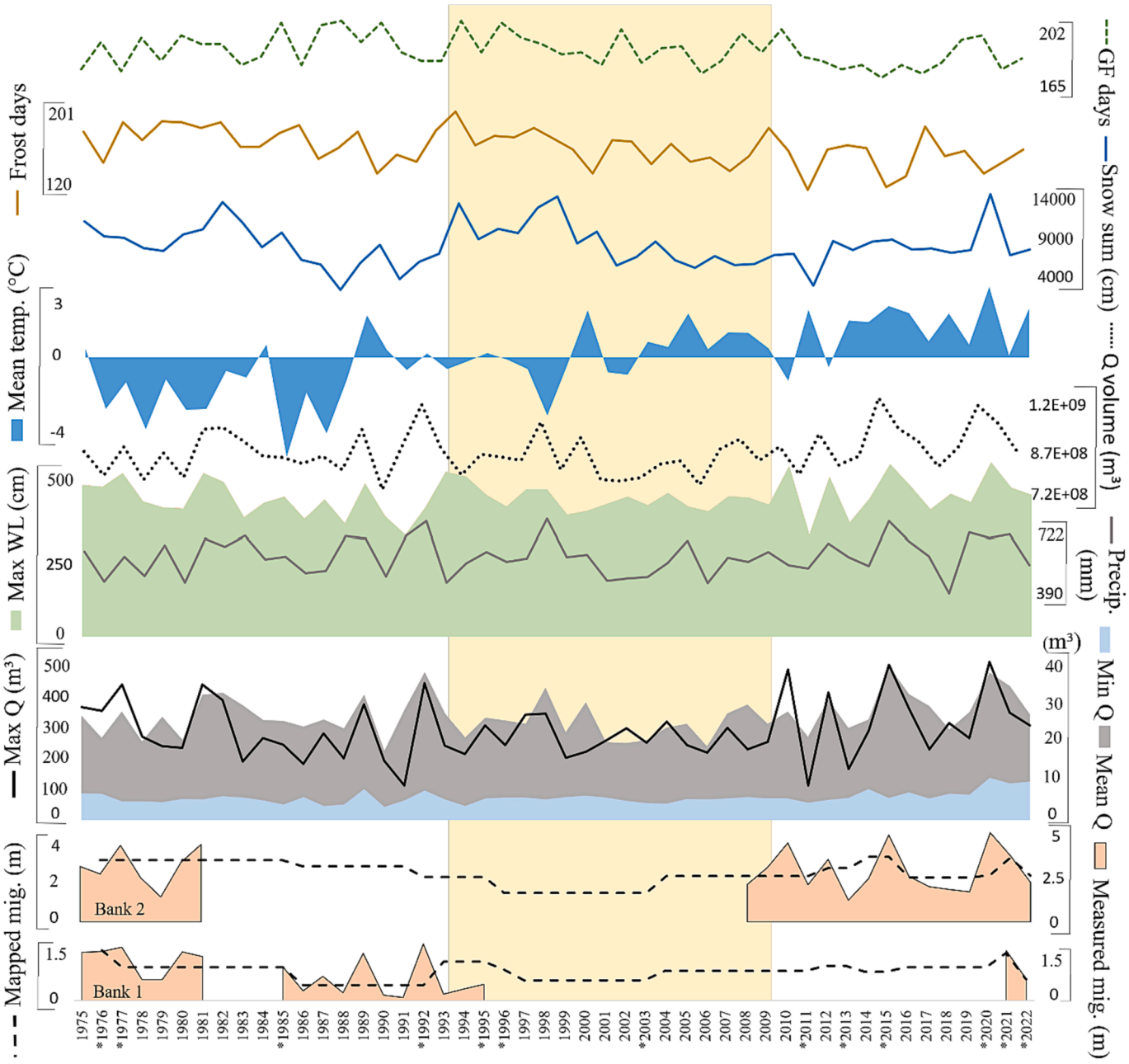

Fig. 8. Time series of the erosion correlated variables plotted. The yellow highlights the period of significant shifts in temperature related variables, and a transition phase where the river system adapted to these changes. During this period low erosion and migration rates were observed together with low spring flood magnitudes, abrupt reduce of winter conditions, and annual mean T shift from < 0 to > 0. The red solid line over migration rate indicates the trend.

happening.

The observed shifts in hydroclimatic variables are expected to have evident impacts on sediment transport and therefore, river morphology. The time span, when the shift in geomorphological variables will be visible in the future, however, is dependent on how the river system adapts to the changing climate. The observed abrupt and rapid changes of temperature and other temperature derived variables have straight impact on discharge, river ice, precipitation and ground frost and therefore to sediment transport, erosion volume and migration rate of the river. Temperature is usually considered as the main factor affecting the sediment transport through altering the discharge and flow conditions (Syvitski, 2002; Walling, 2009; Li et al., 2021). These studies have also highlighted the reduced river ice cover and thickness, increased river flow and runoff during winter, and decreased ground frost as factors increasing the sediment transport. Therefore, we can expect the observed prolongation of thaw-season in spring together with increased winter flow to have an increasing effect on erosion and sediment transport.

The results indicated that spring flood is losing its proportion as part of annual hydrological cycle. This indicates that less erosion and sediment transport takes place during spring flood and if the spring flood will continue to decrease in both, magnitude and proportion, the erosion, migration and sediment transport rates in spring are likely to decrease even more. Similar findings were made in Canadian arctic by Beel et al. (2018) stating that the importance of spring flood as a driver for sediment transport is diminishing. Will the increased erosion potential in other seasons and longer period of sediment being available for transport compensate and equilibrate the diminishing erosion volume of spring, is to be seen.

Zhang et al. (2022) forecasted sediment transport to shift form

temperature-dependent to rain-dependent between 2100 and 2200 in cold regions. For now, the results of this current study indicated slight increase of total erosion and migration. Since most of the correlated parameters were somewhat related to spring or spring flood, it seems that the fragile transition periods from autumn to winter and from winter to spring (thaw-seasons) will have the key role in the future regarding changes in erosion, migration and sediment transport rates. Previous studies (Costa et al., 2018; Li et al., 2021) have also noticed that longer thaw-seasons have potential to increase sediment transport. The fact that most of the observed significant changes in this study took place in November, December, April and May support this conclusion.

Changes in precipitation patterns can contribute to higher runoff and discharge conditions during summer and autumn, potentially leading to increased erosion and sediment transport e.g., Kärkkäinen & Lotsari (2022) reported heavy summer rains leading to increased erosion and sediment transport rates in a Finnish boreal river, reaching almost the intensity of spring flood event. Similar results have been obtained elsewhere in Europe (Costa et al., 2018) and Fennoscandia by Lewis et al. (2012) and Woo (2012) who reported increased summer rainfall and rain intensity causing extreme erosional events and overall increased seasonal sediment yields. Since the erosion volume and migration rate were measured annually every autumn in this study, we cannot detect the seasonal changes from the data, e.g. if the detected increase and intensification of summer rain have increased erosion and sediment transport during summer months, or if the increased base flow during winter has altered the sediment transport pattern and amount during winter.

However, based on the results of this current study and previous studies in similar environments (Beel et al., 2018; Li et al., 2021; Kärkkäinen and Lotsari, 2022; Zhang et al., 2022), we have a reason to predicate the intensified summer rains and increased winter flows to be the cause of slightly increased erosion and migration rates. Thus, we can say that the proportion of erosion and sediment transport during other seasons than spring is increasing and more attention should be addressed to the importance of these factors, often considered as negligible. We did not have any data of suspended sediment loads, and therefore we can't tell if there has been changes in the suspended load of the river. However, studies in Canada, Alpine-Europe and high mountainous Asia (Beel et al., 2018; Costa et al., 2018; Li et al., 2020; Zhang et al., 2023) have reported increased suspended sediment loads together with amplified thaw processes in rivers due to hydrological regime shifts, especially in areas where the sediment load is temperature-determined. This is due to overall increased transport capacity and sediment supply caused by increased summer rain, winter base flow and thawing.

6. Conclusions

Climate change impact on high latitude areas is more evident than on other parts of the world and we expected to detect changes in the temperature, precipitation, and discharge regimes. It is evident that these variables have strong impact on geomorphological processes in fluvial environments. Therefore, if these variables change it means that the geomorphological processes such as sediment transport, erosion, accumulation and hence, the landscape will change. In this study, a time series of hydroclimatic and morphological data was analysed covering the past five decades to determine the possible trends, shifts and correlations between these variables.

The results of this study convince that the effects of climate change on the high latitude areas are already evident: strong signals of warming temperatures indicate reduced winter conditions and warmer summers. Seasonal timing and intensity of precipitation during summer and early winter are changing and the spring flood implication on fluvial systems has diminished as the magnitude has decreased. Simultaneously high discharge peaks have increased in other seasons as well as the annual Min Q.

The analysis of field data over the five decades shows that the meander migration rate and bank erosion volume are interconnected to ground frost, high snow sum, high discharge and water level during spring flood. Thawing has strong control on erosion and sediment transport, and more focus should be addressed on this fragile season since changes of freeze–thaw related variables enhance erosion potential by enabling longer period of sediment availability. Simultaneously, the increased precipitation intensity during summer has the potential to increase erosion and sediment loads.

If the ongoing climate change intensifies and the observed trends continue or even accelerate, it is likely that we will witness shifts in the geomorphological variables as well. How much increased erosion potential in other seasons will compensate the erosion volume and sediment transport capacity lost due to decreased magnitude of spring flood, is something to consider when evaluating possible disturbances on river systems stability in the future. It might be that the magnitude of annual sediment flux remains approximately the same, but the temporal dimensions change when the river system adapts to the hydroclimatic regime shift.

CRediT authorship contribution statement

Linnea Blåfield: Writing – review & editing, Writing – original draft, Visualization, Validation, Methodology, Investigation, Funding acquisition, Formal analysis, Data curation. **Hannu Marttila:** Writing – review & editing, Resources. **Elina Kasvi:** Supervision. **Petteri Alho:** Supervision, Resources, Funding acquisition.

Declaration of competing interest

The authors declare that they have no known competing financial interests or personal relationships that could have appeared to influence the work reported in this paper.

Acknowledgements

This study was conducted as a part of the Fresh Water Competence Centre activities. The study was funded by the European Union - The Next Generation EU recovery instrument (RFF) through Academy of Finland projects Hydro-RI-Platform (346161) and Green-Digi-Basin (347701), by Kone Foundation (202104246), and by Turku University Foundation (080797). Thanks for everyone involved in the field work; Researchers of Fluvial Research Group of University of Turku, Oulanka Research Station and Associate Professor Leo Koutaniemi, University of Oulu. Special thanks to Oulanka Research Station station manager Riku Paavola, to National Land Survey of Finland for the historical data sets, and to the Defence Command of Finland for research permission at the border area.

Appendix

Appendix 1

Main variables T, P, Q, WL and MOR and the sub-variables derived from those. M = monthly analysis, A = annual analaysis.

Main variable	Temperature (C)	Precipitation (mm)	Discharge (m3/s)	Water level (cm)	Morphology
Derived variables	Tmean (M/A)	Total precipitation (M/A)	Mean Q (M/A)	Mean WL (M/A)	Erosion volume Bank 1 (A)
	Tmin(M/A)	P0-5 (M/A)	MinQ (M/A)	MinWL (M/A)	Erosion volume Bank 2 (A)
	Tmax (M/A)	P5-15 (M/A)	Max Q (M/A)	Max WL (M/A)	Migration rate Bank 1 (A)
	DTR (M/A)	P15-25 (M/A)	Q volume (A)	P90 WL (A)	Migration rate Bank 2 (A)
	Frost days (M/A)	P > 25 (M/A)	P90 Q (A)	P90 WL days (annual total)	Net volumetric change Bend 1 (A)
	Frost sum (M/A)	Snow sum (M/A)	Total P90 volume (A)	P90 WL days during spring flood (A)	Net volumetric change Bend 2 (A)
	Freeze-thaw days (M/A)	Snow cover days (M/A)	Spring flood volume (A)	Day of WL > P90 (Spring flood) (A)	
	Ground frost days (M/A)		Total P90% of total Q (A)	Day of WL < P90 (spring flood) (A)	
	Thermal spring start day (A)		Spring flood % of total Q (A)		
			P90 peaks outside spring flood (A)		
			Day of Max Q (A)		
			Day of Q > P90 (spring flood) (A)		
			Day of Q < P90 (spring flood) (A)		
			Flood days total (A)		
			Flood days spring (A)		

Appendix 2

Spearman's correlation and partial correlation between hydroclimatic and morphological variables.

Variable	Spearman correlation	
	Migration rate	Erosion volume
Max Q	0.688	0.663
p90 Q	0.458	0.485
Spring flood volume	0.546	0.532
MinQ	0.315	0.401
Max WL	0.618	0.575
Total number of p90 WL peaks	0.499	0.509
Annual snow sum	0.514	0.540
Number of frost days	0.423	0.415
	Partial correlation (0.95 threshold)	
Number of ground frost days	–	−0.952
Erosion volume	0.953	1
	Partial correlation (0.80 threshold)	
p90 Q volume (m3)	–	0.886
Max Q (m3/s)	–	0.850
Precipitation (mm)	–	0.847
Number of flood days	–	0.884
Number of ground frost days	−0.873	−0.952

References

Ahmed, R., Prowse, T., Dibike, Y., Bonsal, B., O'Neil, H., 2020. Recent trends in freshwater influx to the Arctic Ocean from four major Arctic-draining rivers. Water 12 (4), 1189. https://doi.org/10.3390/w12041189.

Beel, C.R., Lamoureux, S.F., Orwin, J.F., 2018. Fluvial response to a period of hydrometeorological change and landscape disturbance in the Canadian high Arctic. Geophys. Res. Lett. 45 (19), 10–446.

Berghuijs, W., Woods, R., Hrachowitz, M., 2014. A precipitation shift from snow towards rain leads to a decrease in streamflow. Nature Clim Change 4, 583–586. https://doi.org/10.1038/nclimate2246.

Bergström, S., Carlsson, B., Gardelin, M., Lindström, G., Pettersson, A., Rummukainen, M., 2001. Climate change impacts on runoff in Sweden— assessments by global climate models, dynamical downscaling and hydrological modelling.

Bieniek, P.A., Bhatt, U.S., Walsh, J.E., Lader, R., Griffith, B., Roach, J.K., Thoman, R.L., 2018. Assessment of Alaska rain-on-snow events using dynamical downscaling. J. Appl. Meteorol. Climatol. 57, 1847–1863. https://doi.org/10.1175/JAMC-D-17-0276.1.

Blöschl, G., Hall, J., Parajka, J., Perdigão, R.A., Merz, B., Arheimer, B., Živković, N., 2017. Changing climate shifts timing of European floods. Science 357 (6351), 588–590. https://doi.org/10.1126/sciadv.adf8576.

Box, J.E., Colgan, W.T., Christensen, T.R., Schmidt, N.M., Lund, M., Parmentier, F.-J.-W., Brown, R., Bhatt, U.S., Euskirchen, E.S., Romanovsky, V.E., Walsh, J.E., Overland, J. E., Wang, M., Corell, R.W., Meier, W.N., Wouters, B., Mernild, S., Mård, J., Pawlak, J., Olsen, M.S., 2019. Key indicators of Arctic climate change:1971–2017. Environ. Res. Lett. 14, 045010 https://doi.org/10.1088/1748-9326/aafc1b.

Brodu, N., Lague, D., 2012. 3D terrestrial lidar data classification of complex natural scenes using a multi-scale dimensionality criterion: Applications in geomorphology. ISPRS J. Photogramm. Remote Sens. 68, 121–134. https://doi.org/10.1016/j.isprsjprs.2012.01.006.

Brown, D.R., Brinkman, T.J., Verbyla, D.L., Brown, C.L., Cold, H.S., Hollingsworth, T.N., 2018. Changing river ice seasonality and impacts on interior Alaskan communities. Weather Clim. Soc. 10 (4), 625–640. https://doi.org/10.1175/WCAS-D-17-0101.1.

Citakoglu, H., Minarecioglu, N., 2021. Trend analyzis and change point determination for hydro-meteorological and groundwater data of Kizilirmak basin. Theor. Appl. Climatol. 145 (3–4), 1275–1292. https://doi.org/10.1007/s00704-021-03696-9.

Cockburn, J.M., Lamoureux, S.F., 2008. Hydroclimate controls over seasonal sediment yield in two adjacent high Arctic watersheds. Hydrol. Process. Int. J. 22 (12), 2013–2027. https://doi.org/10.1002/hyp.6798.

Costa, A., Molnar, P., Stutenbecker, L., Bakker, M., Silva, T.A., Schlunegger, F., Girardclos, S., 2018. Temperature signal in suspended sediment export from an Alpine catchment. Hydrol. Earth Syst. Sci. 22 (1), 509–528.

Daneshvar Vousoughi, F., Dinpashoh, Y., Aalami, M.T., Jhajharia, D., 2013. Trend analysis of groundwater using non-parametric methods (case study: Ardabil plain). Stochastic Environ. Res. Rsk Assessm. 27, 547–559. https://doi.org/10.1007/s00477-012-0599-4.

De Rose, R.C., Basher, L.R., 2011. Measurement of river bank and cliff erosion from sequential LIDAR and historical aerial photography. Geomorphology 126 (1–2), 132–147. https://doi.org/10.1016/j.geomorph.2010.10.037.
Devito, K., Creed, I., Gan, T., Mendoza, C., Petrone, R., Silins, U., Smerdon, B., 2005. A framework for broad-scale classification of hydrologic response units on the boreal plain: Is topography the last thing to consider? Hydrol. Proces. Int. J. 19 (8), 1705–1714. https://doi.org/10.1002/hyp.5881.
Dinpashoh, Y., Jhajharia, D., Fakheri-Fard, A., Singh, V.P., Kahya, E., 2011. Trends in reference crop evapotranspiration over Iran. J. Hydrol. 399 (3–4), 422–433. https://doi.org/10.1016/j.jhydrol.2011.01.021.
Duan, L., Man, X., Kurylyk, B.L., Cai, T., 2017. Increasing winter baseflow in response to permafrost thaw and precipitation regime shifts in northeastern China. Water 9 (1), 25. https://doi.org/10.3390/w9010025.
Favaro, E.A., Lamoureux, S.F., 2014. Antecedent controls on rainfall runoff response and sediment transport in a high Arctic catchment. Geogr. Ann. Ser. B: Physical Geography 96 (4), 433–446. https://doi.org/10.1111/geoa.12063.
Andrew C. Forbes, Scott F. Lamoureux (2005) Climatic Controls on Streamflow and Suspended Sediment Transport in Three Large Middle Arctic Catchments, Boothia Peninsula, Nunavut, Canada, Arctic, Antarctic, and Alpine Research,37:3, 304-315, 10.1657/1523-0430(2005)037[0304:CCOSAS]2.0.CO;2.
Gohari, A., Shahrood, A.J., Ghadimi, S., Alborz, M., Patro, E.R., Klöve, B., Haghighi, A.T., 2022. A century of variations in extreme flow across finnish rivers. Environ. Res. Lett. 17 (12), 124027 https://doi.org/10.1088/1748-9326/aca554.
Goudie, A.S., 2006. Global warming and fluvial geomorphology. Geomorphology 79 (3–4), 384–394. https://doi.org/10.1016/j.geomorph.2006.06.023.
Gurnell, A.M., 1997. Channel change on the river Dee meanders, 1946–1992, from the analyzis of air photographs. Regulated Rivers: Research & Management: an International Journal Devoted to River Research and Management 13 (1), 13–26. https://doi.org/10.1002/(SICI)1099-1646(199701)13:1<13::AID-RRR420>3.0.CO;2-W.
Hamed, K.H., Rao, A.R., 1998. A modified mann-kendall trend test for autocorrelated data. J. Hydrol. 204 (1–4), 182–196. https://doi.org/10.1016/S0022-1694(97)00125-X.
Hooke, J.M., 2008. Temporal variations in fluvial processes on an active meandering river over a 20-year period. Geomorphology 100 (1–2), 3–13. https://doi.org/10.1016/j.geomorph.2007.04.034.
Hughes, A.O., Huirama, M.K., Owens, P.N., Petticrew, E.L., 2022. Stream bank erosion as a source of sediment within New Zealand catchments. N. Z. J. Mar. Freshw. Res. 56 (4), 632–655. https://doi.org/10.1080/00288330.2021.1929352.
Iman, R.L., Helton, J.C., 1988. An investigation of uncertainty and sensitivity analyzis techniques for computer models. Risk Analysanalyz1 71–90. https://doi.org/10.1111/j.1539-6924.1988.tb01155.x.
IPCC, 2022. Climate Change 2022: Impacts, Adaptation, and Vulnerability. Contribution of Working Group II to the Sixth Assessment Report of the Intergovernmental Panel on Climate Change. In: Pörtner, H.-O., Roberts, D.C., Tignor, M., Poloczanska, E.S., Mintenbeck, K., Alegría, A., Craig, M., Langsdorf, S., Löschke, S., Möller, V., Okem, A., Rama, B. (Eds.), Contribution of Working Group II to the Sixth Assessment Report of the Intergovernmental Panel on Climate. Cambridge University Press, Cambridge, UK and New York, NY, USA, p. 3056. https://doi.org/10.1017/9781009325844.
Irannezhad, M., Ahmadian, S., Sadeqi, A., Minaei, M., Ahmadi, B., Marttila, H., 2022. Peak spring flood discharge magnitude and timing in natural Rivers across northern Finland: Long-term variability, trends, and links to climate teleconnections. Water 14 (8), 1312. https://doi.org/10.3390/w14081312.
Jenicek, M., Seibert, J., Staudinger, M., 2018. Modeling of future changes in seasonal snowpack and impacts on summer low flows in alpine catchments. Water Resour. Res. 54 (1), 538–556. https://doi.org/10.1002/2017WR021648.
Jhajharia, D., Dinpashoh, Y., Kahya, E., Choudhary, R.R., Singh, V.P., 2014. Trends in temperature over Godavari river basin in southern peninsular India. Int. J. Climatol. 34 (5), 1369–1384. https://doi.org/10.1002/joc.3761.
Jokinen, P., Pirinen, P., Kaukoranta, J.-P., Kangas, A., Alenius, P., Eriksson, P., Johansson, M., Wilkman, S., 2021. Tilastoja Suomen Ilmastosta ja Merestä 1991–2020. Ilmatieteen laitos Helsinki.
Jonasson, C., Nyberg, R., 1999. The rainstorm of August 1998 in the Abisko area, northern Sweden: preliminary report on observations of erosion and sediment transport. Geogr. Ann. Ser. B 81 (3), 387–390. https://doi.org/10.1002/joc.3761.
Kasvi, et al., 2013. Morphological changes on meander point bars associated with flow structure at different discharges. ESPL 38, 6. https://doi.org/10.1002/esp.3303.
Kendall, M.G., 1975. Rank Correlation Methods. Charles Griffin, London.
Kersalo, J., Pirinen, P., 2009. Suomen maakuntien ilmasto. Ilmatieteen laitos, Helsinki. Ilmatieteen Laitoksen Raportteja 2009 (8), 185 s.
Kociuba, W., Janicki, G., Siwek, K., Gluza, A. (2012). Bedload transport as an indicator of contemporary transformations of arctic fluvial systems. Monitoring Simulation Prevention and Remediation of Dense and Debris Flows IV; WIT Press: Boston, MA, USA, 125-135. 10.2495/DEB120111.
Korhonen, J., Kuusisto, E., 2010. Long-term changes in the discharge regime in Finland. Hydrol. Res. 41 (3–4), 253–268. https://doi.org/10.2166/nh.2010.112.
Koutaniemi, L., 1979. Late-glacial and post-glacial development of the valleys Oulanka river basin, North-Eastern Finland. Fennia-Int. J. Geogr. 157 (1), 13–73.
Koutaniemi, L., 1984. The role of ground frost, snow cover, ice break-up and flooding in the fluvial processes of the Oulanka river, NE Finland. Fennia-Int. J. Geogr. 162 (2).
Koutaniemi, L., 2000. Meanderointi ja sen yhdentoista vuoden seuranta Oulankajoella Kuusamossa. Terra 112 (4).
Kärkkäinen, M., Lotsari, E., 2022. Impacts of rising, peak and receding phases of discharge events on erosion potential of a boreal meandering river. Hydrol. Process. 36 (10), e14674. https://doi.org/10.1002/hyp.14674.
Lamoureux, S., 2000. Five centuries of interannual sediment yield and rainfall-induced erosion in the Canadian high Arctic recorded in lacustrine varves. Water Resour. Res. 36 (1), 309–318. https://doi.org/10.1029/1999WR900271.
Lane, S.N., Tayefi, V., Reid, S.C., Yu, D., Hardy, R.J., 2007. Interactions between sediment delivery, channel change, climate change and flood risk in a temperate upland environment. Earth Surf. Proc. Land. 32 (3), 429–446. https://doi.org/10.1002/esp.1404.
Lane, S.N., 2013. 21st century climate change: where has all the geomorphology gone? Earth Surf. Proc. Land. 38 (1), 106–110. https://doi.org/10.1002/esp.3362.
Laudon, H., Spence, C., Buttle, J., Carey, S.K., McDonnell, J.J., McNamara, J.P., Tetzlaff, D., 2017. Save northern high-latitude catchments. Nat. Geosci. 10 (5), 324–325. https://doi.org/10.1038/ngeo2947.
Leopold & Wolman, 1960. River meanders. Geol. Soc. Am. Bull. 71, 769–793. https://doi.org/10.1130/0016-7606(1960)71[769:RM]2.0.CO;2.
Lewis, E., Fowler, H., Alexander, L., Dunn, R., McClean, F., Barbero, R., Blenkinsop, S., 2019. GSDR: a global sub-daily rainfall dataset. J. Clim. 32 (15), 4715–4729. https://doi.org/10.1175/JCLI-D-18-0143.1.
Li, S., Xiong, L., Li, H.Y., Leung, L.R., Demissie, Y., 2016. Attributing runoff changes to climate variability and human activities:uncertainty analyzis using four monthly water balance models. Stoch. Env. Res. Risk A. 30, 251–269. https://doi.org/10.1007/s00477-015-1083-8.
Li, D., Li, Z., Zhou, Y., Lu, X., 2020. Substantial increases in the water and sediment fluxes in the headwater region of the Tibetan Plateau in response to global warming. Geophys. Res. Lett. 47 (11) https://doi.org/10.1029/2020GL087745.
Li, D., Overeem, I., Kettner, A.J., Zhou, Y., Lu, X., 2021. Air temperature regulates erodible landscape, water, and sediment fluxes in the permafrost-dominated catchment on the Tibetan Plateau. Water Resour. Res. 57 (2).
Liu, L., Xu, Z.X., Huang, J.X., 2012. Spatio-temporal variation and abrupt changes for major climate variables in the Taihu Basin, China. Stoch. Env. Res. Risk A. 26, 777–791. https://doi.org/10.1007/s00477-011-0547-8.
Lotsari, E., Veijalainen, N., Alho, P., Käyhkö, J., 2010. Impact of climate change on future discharges and flow characteristics of the Tana River, sub-arctic northern Fennoscandia. Geogr. Ann. Ser. B 92 (2), 263–284. https://doi.org/10.1111/j.1468-0459.2010.00394.x.
Lotsari, E., Vaaja, M., Flener, C., Kaartinen, H., Kukko, A., Kasvi, E., Hyyppä, H., Hyyppä, J., Alho, P., 2014. Annual bank and point bar morphodynamics of a meandering river determined by high-accuracy multitemporal laser scanning and flow data. Water Resour. Res. 50, 5532–5559. https://doi.org/10.1002/2013WR014106.
Mann, H.B., 1945. Nonparametric tests against trend. Econometrica 245–259. https://doi.org/10.2307/1907187.
Meriö, L.J., Ala-aho, P., Linjama, J., Hjort, J., Kløve, B., Marttila, H., 2019. Snow to precipitation ratio controls catchment storage and summer flows in boreal headwater catchments. Water Resour. Res. 55 (5), 4096–4109. https://doi.org/10.1029/2018WR023031.
Mustonen, T., Shadrin, V., 2021. The river alazeya. Arctic 74 (1), 67–86. https://doi.org/10.14430/arctic72238.
Nicoll, T.J., Hickin, E.J., 2010. Planform geometry and channel migration of confined meandering rivers on the Canadian prairies. Geomorphology 116 (1–2), 37–47. https://doi.org/10.1016/j.geomorph.2009.10.005.
Niittynen, P., Heikkinen, R.K., Luoto, M., 2018. Snow cover is a neglected driver of Arctic biodiversity loss. Nat. Clim. Chang. 8, 997–1001. https://doi.org/10.1038/s41558-018-0311-x.
Partal, T., Kahya, E., 2006. Trend analyzis in Turkish precipitation data. Hydrol. Process. Int. J. 20 (9), 2011–2026. https://doi.org/10.1002/hyp.5993.
Pettitt, A.N., 1979. A non-parametric approach to the change-point problem. J. Roy. Stat. Soc.: Ser. C (Appl. Stat.) 28 (2), 126–135. https://doi.org/10.2307/2346729.
Pirinen, P., Simola, H., Aalto, J., Kaukoranta, J-P., Karlsson, P., Ruuhela, R. 2012. Tilastoja Suomen ilmastosta 1981–2010. (Climatological statistics of Finland 1981–2010) Ilmatieteen laitos, Helsinki. Ilmatieteen laitoksen raportteja 2012:1. 83 s.
Qin, J., Ding, Y., Han, T., 2020. Quantitative assessment of winter baseflow variations and their causes in Eurasia over the past 100 years. Cold Reg. Sci. Technol. 172, 102989 https://doi.org/10.1016/j.coldregions.2020.102989.
Rantanen, M., Karpechko, A.Y., Lipponen, A., Nordling, K., Hyvärinen, O., Ruosteenoja, K., Vihma, T., Laaksonen, A., 2022. The Arctic has warmed nearly four times faster than the globe since 1979. Commun. Earth Environ. 3, 168. https://doi.org/10.1038/s43247-022-00498-3.
Richard, G.A., Julien, P.Y., Baird, D.C., 2005. Statistical analysis of lateral migration of the Rio Grande, New Mexico. Geomorphology 71 (1–2), 139–155. https://doi.org/10.1016/j.geomorph.2004.07.013.
Salmela, J., Kasvi, E., Vaaja, M.T., Kaartinen, H., Kukko, A., Jaakkola, A., Alho, P., 2020. Morphological changes and riffle-pool dynamics related to flow in a meandering river channel based on a 5-year monitoring period using close-range remote sensing. Geomorphology 352, 106982. https://doi.org/10.1016/j.geomorph.2019.106982.
Sen, P.K., 1968. Estimates of the regression coefficient based on Kendall's tau. J. Am. Stat. Assoc. 63 (324), 1379–1389. https://doi.org/10.1080/01621459.1968.10480934.
Sippel, S., Meinshausen, N., Fischer, E.M., et al., 2020. Climate change now detectable from any single day of weather at global scale. Nat. Clim. Chang. 10, 35–41. https://doi.org/10.1038/s41558-019-0666-7.
Spearman, C., 1906. 'Footrule' for measuring correlation. Br. J. Psychol. 2, 89–108.
St. Jacques, J.M., Sauchyn, D.J., 2009. Increasing winter baseflow and mean annual streamflow from possible permafrost thawing in the Northwest Territories, Canada. Geophys. Res. Lett. 36 (1).

Stocker, T.F., Qin, D., Plattner, G.K., Alexander, L.V., Allen, S.K., Bindoff, N.L., ... Xie, S. P. (2013). Technical summary. In Climate change 2013: the physical science basis. Contribution of Working Group I to the Fifth Assessment Report of the Intergovernmental Panel on Climate Change (pp. 33-115). Cambridge University Press. 10.1029/2008GL035822.

Syvitski, 2002. Sediment discharge variability in Arctic rivers: Implications for a warmer future. Polar Res. 21 (2), 323–330. https://doi.org/10.3402/polar.v21i2.6494.

Thoma, D.P., Gupta, S.C., Bauer, M.E., Kirchoff, C.E., 2005. Airborne laser scanning for riverbank erosion assessment. Remote Sens. Environ. 95 (4), 493–501. https://doi.org/10.1016/j.rse.2005.01.012.

Veijalainen, N., Lotsari, E., Alho, P., Vehviläinen, B., Käyhkö, J., 2010. National scale assessment of climate change impacts on flooding in Finland. J. Hydrol. (Amst) 391, 333–350. https://doi.org/10.1016/j.jhydrol.2010.07.035.

Verstraeten, W.W., Veroustraete, F., van der Sande, C.J., Grootaers, I., Feyen, J., 2006. Soil moisture retrieval using thermal inertia, determined with visible and thermal spaceborne data, validated for European forests. Remote Sens. Environ. 101 (3), 299–314. https://doi.org/10.1016/j.rse.2005.12.016.

Villarini, G., Smith, J.A., 2010. Flood peak distributions for the eastern United States. Water Resour. Res. 46 (6) https://doi.org/10.1029/2009WR008395.

Walling, D.E. (2009). The impact of global change on erosion and sediment transport by rivers: current progress and future challenges.

Wijngaard, J.B., Klein Tank, A.M.G., Können, G.P., 2003. Homogeneity of 20th century European daily temperature and precipitation series. Int. J. Climatol. 23 (6), 679–692. https://doi.org/10.1002/joc.906.

Woo, M.K., Thorne, R., Szeto, K., Yang, D., 2008. Streamflow hydrology in the boreal region under the influences of climate and human interference. Philos. Trans. R. Soc., B: Biological Sci 363 (1501), 2249–2258. https://doi.org/10.1098/rstb.2007.2197.

Wu, Z., Xie, P., Sang, Y.F., Chen, J., Ke, W., Zhao, J., Zhao, Y., 2019. Moving correlation coefficient-based method for jump points detection in hydroclimate time series. Stoch. Env. Res. Risk A. 33, 1751–1764. https://doi.org/10.1007/s00477-019-01727-6.

Xie, H., Li, D., Xiong, L., 2014. Exploring the ability of the Pettitt method for detecting change point by Monte Carlo simulation. Stoch. Env. Res. Risk A. 28, 1643–1655. https://doi.org/10.1007/s00477-013-0814-y.

Zhang, S., Lu, X.X., 2009. Hydrological responses to precipitation variation and diverse human activities in a mountainous tributary of the lower Xijiang. China. Catena 77 (2), 130–142. https://doi.org/10.1016/j.catena.2008.09.001.

Zhang, T., Li, D., East, A.E., Walling, D.E., Lane, S., Overeem, I., Lu, X., 2022. Warming-driven erosion and sediment transport in cold regions. Nat. Rev. Earth Environ. 3 (12), 832–851. https://doi.org/10.1038/s43017-022-00362-0.

Zhang, T., et al., 2023. Shifted sediment-transport regimes by climate change and amplified hydrological variability in cryosphere-fed rivers. Science Advances 9 (45), eadi5019. https://doi.org/10.1126/sciadv.adi5019.